AIP | The Journal of Chemical Physics

Confinement of Ar between two identical parallel semi-infinite walls

Salvador A. Sartarelli and Leszek Szybisz

Citation: The Journal of Chemical Physics **132**, 064701 (2010); doi: 10.1063/1.3306449
View online: http://dx.doi.org/10.1063/1.3306449
View Table of Contents: http://scitation.aip.org/content/aip/journal/jcp/132/6?ver=pdfcov
Published by the AIP Publishing

Articles you may be interested in

Semi-infinite boundary conditions for the simulation of interfaces: The Ar/CO2(s) model revisited
J. Chem. Phys. **136**, 104703 (2012); 10.1063/1.3692608

Full correspondence between asymmetric filling of slits and first-order phase transition lines
AIP Advances **1**, 042146 (2011); 10.1063/1.3664297

Effect of three-body interactions on Ar adsorption on graphitized carbon black
J. Chem. Phys. **132**, 194703 (2010); 10.1063/1.3432451

Density functional approach for modeling CO 2 pressurized polymer thin films in equilibrium
J. Chem. Phys. **130**, 084902 (2009); 10.1063/1.3077861

Symmetry breaking of the fluid density profiles in closed nanoslits
J. Chem. Phys. **126**, 124503 (2007); 10.1063/1.2715934

This article is copyrighted as indicated in the article. Reuse of AIP content is subject to the terms at: http://scitation.aip.org/termsconditions. Downloaded to IP: 157.92.4.75 On: Fri, 26 Jun 2015 19:33:02

Confinement of Ar between two identical parallel semi-infinite walls

Salvador A. Sartarelli[1] and Leszek Szybisz[2,a)]
[1]*Instituto de Desarrollo Humano, Universidad Nacional de General Sarmiento, Gutierrez 1150, San Miguel RA-1663, Argentina*
[2]*Departamento de Física, Comisión Nacional de Energía Atómica, Laboratorio TANDAR, Av. del Libertador 8250, Buenos Aires RA-1429, Argentina; Departamento de Física, Facultad de Ciencias Exactas y Naturales, Universidad de Buenos Aires, Ciudad Universitaria, Buenos Aires RA-1428, Argentina; and Consejo Nacional de Investigaciones Científicas y Técnicas, Av. Rivadavia 1917, Buenos Aires RA-1033, Argentina*

(Received 13 November 2009; accepted 12 January 2010; published online 11 February 2010)

The confinement of Ar in planar slits of two identical parallel semi-infinite walls of alkali metals, alkaline-earth metal Mg, and CO_2 is investigated within the framework of the density functional theory. It is assumed that (1) the fluid atoms interact via a recently proposed effective attractive pair potential with strength, ε_{ff}, which reproduces the experimental data of the surface tension of the liquid-vapor interface at the bulk coexistence curve, and (2) the adsorption on the walls is described by *ab initio* potentials characterized by a well depth, $\mathcal{W}_{sf}$. In this way the systems were studied in the framework of a realistic approach. We found that for small coverages, the slit is always filled by forming two symmetric vapor films, one at each wall. For increasing coverage the behavior depends on the ratio $\mathcal{W}_{sf}/\varepsilon_{ff}$ and the temperature T. In the case of alkali metals, we found at the triple point, T_t, of the adsorbate a regime of average density ρ^*_{av} in which the ground state exhibits asymmetric density profiles, leading to the so-called spontaneous symmetry breaking (SSB) effect. The SSB appears at an average density ρ^*_{sb1} and disappears at a higher average density ρ^*_{sb2}. When T is increased, the range of densities $\rho^*_{\mathrm{sb1}} \leq \rho^*_{\mathrm{av}} \leq \rho^*_{\mathrm{sb2}}$ diminishes and eventually the SSB disappears at a critical temperature, T_{sb}, which coincides with the critical prewetting temperature T_{cpw} observed in the adsorption on a single wall. For $T > T_{\mathrm{cpw}}$ the slit is filled symmetrically up to the phase transition to capillary condensation. All these features are examined as a function of the strength of the substrate and the width of the slit. Furthermore, no SSB effect was found for Mg and CO_2. © *2010 American Institute of Physics*. [doi:10.1063/1.3306449]

I. INTRODUCTION

The study of the physisorption of fluids on solid substrates led to very fascinating phenomena mainly determined by the relative strengths of fluid-fluid (*f-f*) and substrate-fluid (*s-f*) attractions, ε_{ff} and $\mathcal{W}_{sf}$, respectively.[1] An interesting tour from adsorption on a single wall toward confinement in a slit geometry is described in Ref. 2. In that letter, Rascón and Parry present a simple theoretical model which smoothly connects wetting and capillary condensation, showing the rich sequence of different regimes and phenomena induced by the substrate shape. In the present work we shall mainly refer to properties of fluids confined between two identical planar parallel semi-infinite walls. We consider structureless walls which define a *x-y* plane. It is usually assumed that the density profile $\rho(\mathbf{r})$ of the fluid is invariant on this plane depending only on the coordinate z perpendicular to the walls. About 20 years ago, van Leeuwen and co-workers carried out calculations for simple fluids confined in such a slit geometry on the Delf molecular dynamics (MD) processor, which was designed *ad hoc* for MD simulations of this kind of system.[3,4] It was assumed that the atoms of the fluid interact via standard Lennard-Jones (LJ) potentials with strength ε_{ff} and size σ_{ff} parameters. The width of the slit was $L=29.1\sigma_{ff}$, which is sufficiently large to avoid any capillary effect and support solid-liquid (*s-l*), solid-vapor (*s-v*), and liquid-vapor (*l-v*) interfaces. The results for reduced temperature $T^*=k_BT/\varepsilon_{ff}=0.9$, which lies between the triple point temperature $T^*_t \simeq 0.7$ and the critical point temperature $T^*_c \simeq 1.3$ of the bulk adsorbate, were published in a series of papers of the Delf collaboration.[5–9] These authors found that the behavior depends on the ratio $\varepsilon_r=\mathcal{W}_{sf}/\varepsilon_{ff}$. Starting from $\varepsilon_r \simeq 0.1$ they obtained that for increasing ε_r the profiles of the ground state were sequentially (i) symmetric with absence of liquid close to the walls (drying), (ii) asymmetric with liquid at one wall and vapor at the other (incomplete or partial wetting), and (iii) symmetric with liquid at both walls (complete wetting). These structures can be understood in terms of the balance of surface tensions at the *s-l*, *s-v*, and *l-v* interfaces, i.e., γ_{sl}, γ_{sv}, and γ_{lv}, respectively.[5] We shall come back to the latter point in a next section. Now, we shall only mention that the occurrence of the asymmetric profiles of point (ii) is known in the literature as the spontaneous symmetry breaking (SSB) effect.

The works of Berim and Ruckenstein[10,11] renewed the interest in searching for the SSB effect in real systems. These authors studied in Ref. 11 the confinement of Ar in a closed slit composed of two identical walls of CO_2 assuming that the *s-f* interaction is given by the 9-3 potential proposed by

a)Electronic mail: szybisz@tandar.cnea.gov.ar.

 © 2010 American Institute of Physics

This article is copyrighted as indicated in the article. Reuse of AIP content is subject to the terms at: http://scitation.aip.org/termsconditions. Downloaded to IP: 157.92.4.75 On: Fri, 26 Jun 2015 19:33:02

TABLE I. Properties of Ar confined in slits with wall of alkali metals, Mg, and CO_2. The ratio $\mathcal{W}_{sAr}/\varepsilon_{ArAr}$, wetting T_w, and critical prewetting T_{cpw} temperatures are listed. C indicates continuous growth at $T \geq T_t$ and PW denotes present work.

		T_w (K)		T_{cpw} (K)	T_{sb} (K)
Wall	$\mathcal{W}_{sAr}/\varepsilon_{ArAr}$	Expt.[a]	DF[b]	DF[b]	DF[PW]
Cs	1.1				
Rb	1.1		138.7	$141 \leftrightarrow 142$	141.3
K	1.2		137.7	$140 \leftrightarrow 141$	140.3
Na	1.6		124.8	$130 \leftrightarrow 131$	130.1
Li	2.1		110.0	$118 \leftrightarrow 119$	118.4
Mg	3.5		C	C	
CO_2	3.8	C	C	C	

[a]Experimental data from Ref. 17.
[b]Critical prewetting temperatures taken from Ref. 20.

Ebner and Saam.[12] They analyzed a slit of width $L=15\sigma_{ff}$ and stated that SSB occurs for temperatures below a critical value $T_{sb}=106$ K. In a revisited study of this system reported in Ref. 13, we found that the conditions for the occurrence of SSB had been fulfilled in Ref. 11 because the well depth of the *s-f* attraction was diminished by the presence of an extra hard-wall repulsion. In looking for SSB in other systems, we found that inert gases confined in slits of alkali metals exhibit suitable ratios ε_r for the appearance of this effect. Preliminary results for Ne and Ar confined in such a type of slits have recently been reported elsewhere.[14,15]

In the present work we shall report on a rather comprehensive investigation about the behavior of Ar confined in slits of two identical planar walls. The calculations have been carried out within the density functional (DF) theory. The adsorption is described by using the *ab initio s-f* potentials of Ref. 16 for alkaline walls and of Refs. 17 and 18 for CO_2. In order to study the wetting properties of all the above mentioned substrates, the computational task must be performed over the entire temperature range between T_t and T_c of the adsorbate. For this purpose, a recently published proposal[19] for the mean-field approximation (MFA) of the attractive part of the *f-f* interaction was adopted. This effective potential gives a satisfactory description of the surface tension of the liquid-vapor interface, γ_{lv}, of Ar at coexistence for temperatures in the whole range $T_t \leftrightarrow T_c$.[15,20] The behavior of the systems was studied as a function of the width of the slits. It was found that in the cases of alkali metals (Cs, Rb, K, Na, and Li) the SSB effect occurs at temperatures lower than certain critical values T_{sb}. In the present paper, we shall present detailed results for Rb, Na, and Li sweeping the entire range of attraction strengths of the alkali metals (see Table I). On the other hand, the SSB effect does not occur for the stronger attractors Mg and CO_2.

It is known that the isotherms for the adsorption on single planar walls which exert an attraction of moderate strength [i.e., $0.7 \lesssim \varepsilon_r \lesssim 2.5$] exhibit a first-order wetting transition at the point $[T_w, \mu_w = \mu_0(T_w)]$ between T_t and T_c. T_w is characterized by the appearance of coexisting thin and very thick adsorbed fluid films, while for $T < T_w$ the coverage of adsorbed films is finite. Under these conditions for $T \geq T_w$ there is an associated prewetting line in the $\mu - T$ plane.[21] The locus of these prewetting lines extends away from (T_w, μ_w) into the region of pressures below the corresponding bulk saturation value $P_0(T)$ and terminates at the surface critical point (T_{cpw}, μ_{cpw}). A typical phase diagram of the prewetting phenomenon in the $T-\mu$ plane is depicted in Fig. 5 of Ref. 19. In order to get a deeper insight of the SSB effect, we analyzed the correlation between the values of T_{sb} obtained in the present work and the T_{cpw} determined in a recent study of the adsorption of Ar on single walls performed by utilizing exactly the same MFA.[15,20]

The paper is organized in the following way. The theoretical background is summarized in Sec. II. The results together with their analysis are given in Sec. III. Section IV is devoted to the conclusions.

II. THEORETICAL BACKGROUND

Let us first outline the utilized DF formalism and the MFA adopted for describing the attractive part of the *f-f* interaction. Next we shall give the equations used for determining the density profile.

A. Density functional theory

In a DF theory the Helmholtz free energy F_{DF} of an inhomogeneous fluid embedded in an external potential $U_{sf}(\mathbf{r})$ is expressed as a functional of the local density $\rho(\mathbf{r})$ (see, e.g., Refs. 22 and 23),

$$F_{DF}[\rho(\mathbf{r})] = \nu_{id} k_B T \int d\mathbf{r} \rho(\mathbf{r}) \{\ln[\Lambda^3 \rho(\mathbf{r})] - 1\} + \int d\mathbf{r} \rho(\mathbf{r}) f_{HS}[\bar{\rho}(\mathbf{r}); d_{HS}] + \frac{1}{2} \int \int d\mathbf{r} d\mathbf{r}' \rho(\mathbf{r}) \rho(\mathbf{r}'') \Phi_{attr}(|\mathbf{r} - \mathbf{r}'|) + \int d\mathbf{r} \rho(\mathbf{r}) U_{sf}(\mathbf{r}). \quad (2.1)$$

The first term is the ideal gas free energy, where k_B is the Boltzmann constant, Λ is the de Broglie thermal wavelength,

This article is copyrighted as indicated in the article. Reuse of AIP content is subject to the terms at: http://scitation.aip.org/termsconditions. Downloaded to IP: 157.92.4.75 On: Fri, 26 Jun 2015 19:33:02

and ν_{id} is a free parameter introduced in Eq. (2) of Ref. 23 (in the standard theory it is equal unity). The second term accounts for the repulsive *f-f* interaction approximated by a hard-sphere (HS) functional; we utilized the $f_{\mathrm{HS}}[\bar{\rho}(\mathbf{r});d_{\mathrm{HS}}]$ developed by Kierlik and Rosinberg,[24] where $\bar{\rho}(\mathbf{r})$ is an properly averaged density and d_{HS} is the HS diameter. The third term is the attractive *f-f* interactions, treated in a MFA manner. Finally, the last integral represents the effect of the external potential $U_{sf}(\mathbf{r})$ exerted on the fluid.

The attractive part of the *f-f* interaction was described by an effective pair interaction devised in Ref. 19 by using the separation of the LJ potential of Weeks, Chandler, and Andersen,[25]

$$\Phi_{\mathrm{attr}}^{\mathrm{WCA}}(r)=\begin{cases}-\tilde{\varepsilon}_{ff}, & r\le r_m\\ 4\tilde{\varepsilon}_{ff}\left[\left(\dfrac{\tilde{\sigma}_{ff}}{r}\right)^{12}-\left(\dfrac{\tilde{\sigma}_{ff}}{r}\right)^{6}\right], & r>r_m\end{cases}, \tag{2.2}$$

where $r_m=2^{1/6}\tilde{\sigma}_{ff}$ is the position of the LJ minimum. No cutoff radius was introduced for the pair potential. The well depth $\tilde{\varepsilon}_{ff}$ and the interaction size $\tilde{\sigma}_{ff}$ are considered as free parameters because the use of bare values $\varepsilon_{\mathrm{ArAr}}/k_B=119.76$ K and $\sigma_{\mathrm{ArAr}}=3.405$ Å, overestimates the experimental result $T_c=150.86$ K. The latter effect may be observed in Fig. 2 of Ref. 22, which shows the phase envelopes for several approaches. This drawback is mainly due to the fact that the integral $\int_0^\infty r^2dr\Phi_{\mathrm{attr}}^{\mathrm{WCA}}(r)=-(32\sqrt{2}\pi/9)\varepsilon_{\mathrm{ArAr}}\sigma_{\mathrm{ArAr}}^3$ evaluated with the bare parameters becomes too negative. The determined ratios $\tilde{\varepsilon}_{\mathrm{ArAr}}/\varepsilon_{\mathrm{ArAr}}$ and $\tilde{\sigma}_{\mathrm{ArAr}}/\sigma_{\mathrm{ArAr}}$ are slightly smaller than unity.

In summary, the complete DF formalism has three adjustable parameters (namely, ν_{id}, $\tilde{\varepsilon}_{ff}$, and $\tilde{\sigma}_{ff}$), which were determined by imposing that at *l-v* coexistence the pressure as well as the chemical potential of the bulk *l* and *v* phases should be equal [i.e., $P(\rho_l)=P(\rho_v)$ and $\mu(\rho_l)=\mu(\rho_v)$]. In practice, we set $d_{\mathrm{HS}}=\tilde{\sigma}_{ff}$ and at a given temperature T imposed that the coexistence data of ρ_l, ρ_v, and $P(\rho_l)=P(\rho_v)=P_0$ for Ar quoted in Table X of Ref. 26 be reproduced. The procedure is described in Ref. 19. Close to T_t, the values obtained for the parameter ν_{id} are compatible with unity, while near T_c they become about 0.9 accounting for the complicated interactions in the regime where the liquid and vapor densities are of the same order.

The DF formulation outlined above not only provides an adjusted bulk equation of state at saturation, but, in addition, it predicts reasonable values of γ_{lv} at liquid-vapor coexistence. As reported in Refs. 15 and 20, these results are in good agreement over the entire range of temperatures $T_t\le T\le T_c$, with the experimental data for Ar tabulated by Wu and Yan.[27] Moreover, Fig. 2(b) in Ref. 20 indicates that (i) the present DF results are similar to the MD values obtained by Trokhymchuk and Alexandre[28] and (ii) the largest difference with experimental data occurs close to T_t amounting 10%. Therefore, the present MFA becomes an appropriate realistic approach for studying the adsorption of Ar.

B. Euler–Lagrange equations

The equilibrium density profile $\rho(\mathbf{r})$ of the adsorbed fluid is determined by a minimization of the free energy with respect to density variations with the constraint of a fixed number of particles N,

$$\frac{\delta}{\delta\rho(\mathbf{r})}\left[F_{\mathrm{DF}}[\rho(\mathbf{r})]-\mu\int d\mathbf{r}\rho(\mathbf{r})\right]=0. \tag{2.3}$$

Here the Lagrange multiplier μ is the chemical potential of the system. In the case of a planar symmetry where the flat walls exhibit an infinite extent in the x and y directions, we assume that the profile depends only on the coordinate z perpendicular to the substrate. For this geometry, the variation of Eq. (2.3) yields the following Euler-Lagrange (EL) equation:

$$\frac{\delta[(F_{\mathrm{id}}+F_{\mathrm{HS}})/A]}{\delta\rho(z)}+\int_0^L dz'\rho(z')\bar{\Phi}_{\mathrm{attr}}(|z-z'|)+U_{sf}(z)=\mu, \tag{2.4}$$

where

$$\frac{\delta(F_{\mathrm{id}}/A)}{\delta\rho(z)}=\nu_{\mathrm{id}}k_BT\ln[\Lambda^3\rho(z)], \tag{2.5}$$

and

$$\frac{\delta(F_{\mathrm{HS}}/A)}{\delta\rho(z)}=f_{\mathrm{HS}}[\bar{\rho}(z);d_{\mathrm{HS}}]+\int_0^L dz'\rho(z')\frac{\delta f_{\mathrm{HS}}[\bar{\rho}(z');d_{\mathrm{HS}}]}{\delta\bar{\rho}(z')}\frac{\delta\bar{\rho}(z')}{\delta\rho(z)}. \tag{2.6}$$

Here F_{id}/A and F_{HS}/A are free energies per unit area of one wall A and L is the width of the slit. The final EL equation may cast into the form

$$\nu_{\mathrm{id}}k_BT\ln[\Lambda^3\rho(z)]+Q(z)=\mu, \tag{2.7}$$

where

$$Q(z)=f_{\mathrm{HS}}[\bar{\rho}(z);d_{\mathrm{HS}}]+\int_0^L dz'\rho(z')\frac{\delta f_{\mathrm{HS}}[\bar{\rho}(z');d_{\mathrm{HS}}]}{\delta\bar{\rho}(z')}\frac{\delta\bar{\rho}(z')}{\delta\rho(z)}+\int_0^L dz'\rho(z')\bar{\Phi}_{\mathrm{attr}}(|z-z'|)+U_{sf}(z). \tag{2.8}$$

The number of particles N per unit wall's area A is

$$N_s=\frac{N}{A}=\int_0^L\rho(z)dz. \tag{2.9}$$

In order to get solutions for $\rho(z)$ it is useful to rewrite Eq. (2.7) as

$$\rho(z)=\rho_0\exp\left(-\frac{Q(z)}{\nu_{\mathrm{id}}k_BT}\right), \tag{2.10}$$

with

$$\rho_0=\frac{1}{\Lambda^3}\exp\left(\frac{\mu}{\nu_{\mathrm{id}}k_BT}\right). \tag{2.11}$$

This article is copyrighted as indicated in the article. Reuse of AIP content is subject to the terms at: http://scitation.aip.org/termsconditions. Downloaded to IP: 157.92.4.75 On: Fri, 26 Jun 2015 19:33:02

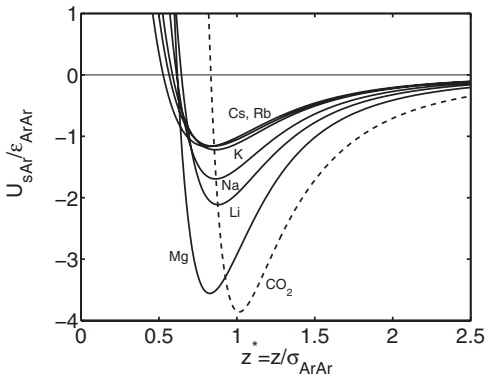

FIG. 1. Reduced adsorption potentials exerted on Ar atoms by the left wall of the slit. Solid curves are CCZ potentials (Ref. 16) for alkali substrates, while the dashed curve stands for the interaction between Ar and a wall of CO_2 from Refs. 17 and 18.

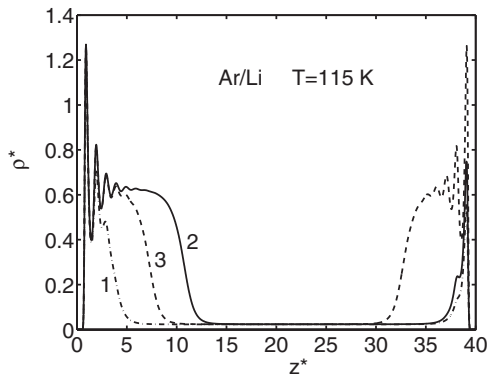

FIG. 2. Density profiles of Ar confined in a slit of Li with $L^*=40$ at $T=115$ K. The displayed spectra denoted by 1, 2, and 3 correspond to average densities $\rho^*_{\rm av}=0.074$, 0.192, and 0.218, respectively.

The relation between μ and N_s is obtained by substituting Eq. (2.10) into the constraint of Eq. (2.9),

$$\mu = -\nu_{\rm id} k_B T \times \ln\left[\frac{1}{N_s \Lambda^3}\int_0^L dz\, \exp\left(-\frac{Q(z)}{\nu_{\rm id} k_B T}\right)\right]. \quad (2.12)$$

When solving this kind of system it is usual to define dimensionless variables $z^*=z/\tilde{\sigma}_{ff}$ for the distance and $\rho^*=\rho\tilde{\sigma}^3_{ff}$ for the densities. In these units the box size becomes $L^*=L/\tilde{\sigma}_{ff}$.

III. RESULTS AND ANALYSIS

The confinement of Ar atoms in a planar slit is governed by the total potential

$$U_{sf}(z) = U_{ab\ initio}(z) + U_{ab\ initio}(L-z), \quad (3.1)$$

where the contributions $U_{ab\ initio}(z)$ are potentials exerted by single walls. For the analysis of confinement between alkaline walls, we adopted in all the cases the *ab initio* potentials of Chismeshya, Cole, and Zaremba[16] (CCZ) with parameters listed in Table I therein. The study of the Ar/CO_2 system was accomplished by utilizing the *s-f* interaction adopted by Mistura *et al.*[17] The latter potential was evaluated in terms of *ab initio* contributions derived by Marshall *et al.*[18] (hereafter referred as M-M potential) and is more realistic than the widely used in the literature 9-3 potential proposed by Ebner and Saam[12] (ES). Figure 1 shows a comparison of the reduced adsorption potentials $U_{ab\ initio}(z)/\varepsilon_{\rm ArAr}$ corresponding to the different examined substrates. Although the M-M and ES potentials for Ar/CO_2 have already been compared in Fig. 3 of Ref. 17, we find convenient to mention here the main differences. The asymptotic behavior in both cases is proportional to $1/z^3$, but the M-M potential exhibits a softer repulsion than the ES one. Moreover, the well depths located at the corresponding z_m differ significantly one from the other being $U_{ab\ initio}(z_m)/\varepsilon_{\rm ArAr}=-3.86$ and $U_{\rm ES}(z_m)/\varepsilon_{\rm ArAr}=-2.78$. Due to this sizable difference an analysis similar to that performed in Ref. 20 leads to different results for $T_{\rm cpw}$, the M-M potential yields complete wetting at T_t without any prewetting line, while the ES one gives a prewetting line with a $T_{\rm cpw}$ about 15 K above T_t.

In the present work we shall report results obtained for slits of widths $L^*=10$, 20, 40, and 60. The slits with walls located at $L^*=20$ and 40 are just equal to that utilized by Maciołek, Evans, and Wilding[29] in their study of a capillary condensed LJ fluid confined in slits by means of a DF theory. These widths guarantee that the pair interaction between two atoms located at different walls is negligible, and that with $L^*=60$ it is even larger. The slit with $L^*=10$ is wider than twice the radius cutoff $r^*_c=2.5$ usually adopted in MD and Monte Carlo calculations and was analyzed to search for size effects. The solutions of the EL equations were calculated at fixed average densities defined in terms of N and L as $\rho^*_{\rm av}=N_s\tilde{\sigma}^3_{ff}/L=N^*_s/L^*$. The calculations were carried out by setting the reduced step of the discretization at $\Delta z^*=\Delta z/\tilde{\sigma}_{\rm ArAr}=0.025$. By iterating self-consistently the set of connected Eqs. (2.7)–(2.12) one always gets the ground-state (g-s) solution, obtaining a good convergence which may be improved by increasing the number of iterations. Asymmetric g-s occurs in a closed range of average densities $\rho^*_{\rm sb1}\le\rho^*_{\rm av}\le\rho^*_{\rm sb2}$. In the regime of $\rho^*_{\rm av}$ where asymmetric profiles exhibit the lowest free energy, one may obtain symmetric solutions by imposing explicitly a symmetric $\rho(z)$ in the whole chain of equations.

A. Symmetry of density profiles

Let us begin the description of the analysis by reporting the results obtained for Ar confined between walls of Li. For temperatures below $T_w=110$ K we obtained large ranges of $\rho^*_{\rm av}$ where the asymmetric solutions exhibit a lower free energy than the corresponding symmetric ones. In spite of the fact that there is a general idea that a connection exists between the SSB effect and nonwetting, we found, by contrast, that the SSB behavior extends above the wetting temperature. The adsorption of Ar on a single planar substrate of Li exhibits a prewetting line which extends over about 10 K from $T_w=110$ to $T_{\rm cpw}\le 119$ K;[15,20] this feature allows for a detailed study of asymmetric solutions above T_w.

Let us first show the sorts of solutions with lowest free energy which may be obtained for this kind of systems and, subsequently, to describe the main results of our work. Figure 2 shows three examples of g-s solutions determined at $T=115$ K (larger than T_w) for a slit of $L^*=40$. These results were obtained by increasing coverage and are the common

This article is copyrighted as indicated in the article. Reuse of AIP content is subject to the terms at: http://scitation.aip.org/termsconditions. Downloaded to IP: 157.92.4.75 On: Fri, 26 Jun 2015 19:33:02

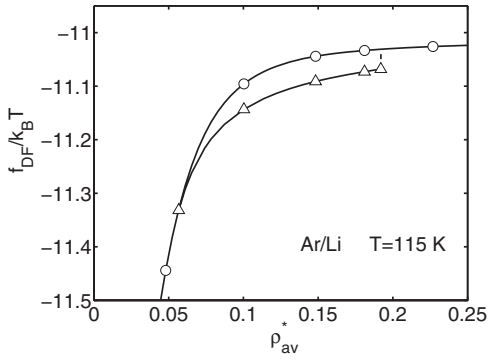

FIG. 3. Reduced free energy per particle of Ar confined in a slit of Li with $L^*=40$ at $T=115$ K displayed as a function of the average density. The curve labeled by circles corresponds to symmetric solutions, that labeled by triangles corresponds to asymmetric ones, and the vertical dashed line at $\rho^*_{av}=0.192$ indicates the end of ground states with asymmetric profiles.

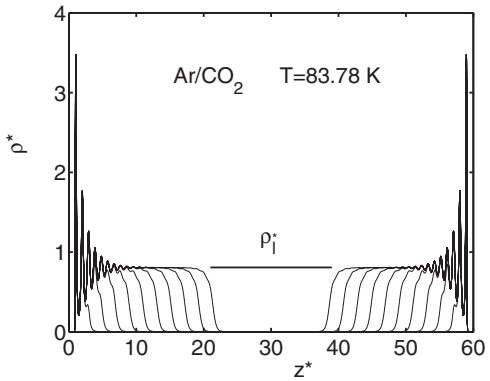

FIG. 4. Density profiles of Ar confined in a slit of CO_2 with $L^*=60$ at T_t. The displayed spectra correspond to average densities ρ^*_{av} ranging from 0.0555 to 0.555 with a constant step. The horizontal line is the liquid density $\rho^*_l=0.808$ at saturation for T_t.

pattern for alkali metals. In this geometry, the repulsion at the walls causes that the profiles at contact, $\rho^*(z^*=0)$ and $\rho^*(z^*=L^*)$, both be equal zero. The result labeled by 1 (dash-dotted curve) is a small asymmetric profile and that labeled by 2 (solid curve) is the largest asymmetric solution at this temperature; both cases are examples of partial wetting. By further increasing ρ^*_{av} the SSB effect disappears and the g-s becomes symmetric (complete wetting) as indicated by the curve labeled by 3 (dashed curve).

Figure 3 shows the free energy per particle, $f_{DF}=F_{DF}/N$ in units of k_BT, for both symmetric and asymmetric solutions for the Ar/Li system at $T=115$ K as a function the average density. According to this picture the g-s exhibits asymmetric profiles between a lower and an upper limit $\rho^*_{sb1}=0.057\leq\rho^*_{av}\leq\rho^*_{sb2}=0.192$. Out of this range no asymmetric solutions were from the set of Eqs. (2.7)–(2.12). For higher temperatures up to $T=118$ K the range $\rho^*_{sb1}\leq\rho^*_{av}\leq\rho^*_{sb2}$ diminishes as the temperature increases. For $T\geq 119$ K the profiles corresponding to the g-s are always symmetric. The same qualitative pattern is exhibited by solutions for slits with other widths.

The slits built of alkali metals heavier than Li exert a weaker attraction on Ar atoms. This feature can be seen in Fig. 1 and Table I. The smaller values of ε_r favor the occurrence of asymmetric g-s. In practice, for the remaining alkali metals we obtained a qualitatively similar behavior to that found for Li. The size of the asymmetry will be discussed in the next subsection.

The conditions for the occurrence of a partial (one wall) wetting or a complete (two walls) wetting can be expressed in terms of the balance of γ_{sl}, γ_{sv}, and γ_{lv} surface tensions. Since such a behavior was carefully discussed in previous works,[5,8,13] here we shall restrict ourselves to briefly outline the main features. When the liquid is adsorbed symmetrically like in the case of profile 3 in Fig. 2, there are two *s-l* and two *l-v* interfaces. Hence, the total surface excess energy may be written as

$$\gamma^{\rm sym}_{\rm tot}=2\gamma_{sl}+2\gamma_{lv}. \tag{3.2}$$

On the other hand, for an asymmetric profile $\gamma^{\rm asy}_{\rm tot}$ becomes

$$\gamma^{\rm asy}_{\rm tot}=\gamma_{sl}+\gamma_{lv}+\gamma_{sv}. \tag{3.3}$$

The three quantities of the right hand side of this equation are related by Young's law [see, e.g., Eq. (2.1) in Ref. 30],

$$\gamma_{sv}=\gamma_{sl}+\gamma_{lv}\cos\,\theta, \tag{3.4}$$

where θ is the contact angle defined as the angle between the wall and the interface between the liquid and the vapor (see Fig. 1 in Ref. 30). By using Young's law, Eq. (3.3) may be rewritten as

$$\gamma^{\rm asy}_{\rm tot}=2\gamma_{sl}+\gamma_{lv}(1+\cos\,\theta), \tag{3.5}$$

with $\cos\,\theta=(\gamma_{sv}-\gamma_{sl})/\gamma_{lv}<1$. If one changes γ_{sl} by increasing enough N_s (as shown in Fig. 3), and/or T, and/or the strength of $U_{sf}(z)$ eventually the equality $\gamma_{sv}-\gamma_{sl}=\gamma_{lv}$ may be reached yielding $\cos\,\theta=1$. Then the system would undergo a transition to a symmetric profile where both walls of the slit are wet.

It is important to remark that, indeed, there are two degenerate asymmetric solutions. Besides that shown in Fig. 2 where the profiles exhibit the thicker film adsorbed on the left wall [left asymmetric solution (LAS)], there is an asymmetric solution with exactly the same free energy but where the thicker film is located near the right wall [right asymmetric solution (RAS)].

On the other hand, Fig. 1 indicates that the adsorption potentials exerted by walls of Mg and CO_2 are significantly more attractive than that of Li, the strongest of alkali metals. This feature causes that already at T_t the filling of slits built of Mg and CO_2 is accomplished by the formation of symmetric profiles. Figure 4 shows a sequence of profiles for increasing average density ρ^*_{av} from 0.0555 to 0.555 for the Ar/CO_2 system at T_t. This behavior is in agreement the wetting at T_t found in Ref. 20.

B. Asymmetry coefficient

The asymmetry of density profiles may be measured by the quantity

This article is copyrighted as indicated in the article. Reuse of AIP content is subject to the terms at: http://scitation.aip.org/termsconditions. Downloaded to IP: 157.92.4.75 On: Fri, 26 Jun 2015 19:33:02

$$\Delta_N = \frac{1}{N_s}\int_0^{L/2} dz[\rho(z) - \rho(L-z)]. \quad (3.6)$$

According to this definition, if the profile is completely asymmetrical about the middle of the slit, i.e., for (i) $\rho(z<L/2)\neq 0$ and $\rho(z\geq L/2)=0$, or (ii) $\rho(z<L/2)=0$ and $\rho(z\geq L/2)\neq 0$, this quantity becomes +1 or −1, respectively, while for symmetric solutions it vanishes.

The asymmetry coefficients Δ_N were evaluated for all the determined solutions. We shall first describe in detail the results for slits of Li and, next, refer to slits of other substrates. Figure 5 shows Δ_N for LAS profiles as a function of ρ^*_{av}. The results for $L^*=10$, 20, 40, and 60 are displayed in four different panels. Data for several values of T are included in each panel. The temperatures are $T=T_t=83.78$ K, $T=109$ K [just below $T_w(\mathrm{Ar/Li})=110.0$ K], and five values above T_w, namely, $T=114$, 115, 116, 117, and 118 K. One may observe that in all these panels the range where asymmetric solutions occur, i.e., $\rho^*_{sb1}\leq\rho^*_{av}\leq\rho^*_{sb2}$, diminishes with increasing temperatures. The SSB effect always disappears at $T=119$ K, which is the upper limit for T_{cpw} determined in Refs. 15 and 20 for the adsorption of Ar on a single wall of Li (see Table I). In addition, Fig. 5 indicates that the range $\rho^*_{sb1}\leq\rho^*_{av}\leq\rho^*_{sb2}$ at a given T, close to T_{cpw}, becomes narrower and moves toward smaller ρ^*_{av} when L^* is increased. It is expected that for even wider slits the data for $T=114$ K will approach that of $T=115$ K.

In order to illustrate the results obtained for Na and Rb, we report the asymmetry coefficients for slits of $L^*=60$. Figure 6 shows Δ_N for LAS profiles in a slit of Na as a function of ρ^*_{av}. The displayed data correspond to the following temperatures: $T=T_t$, $T=124$ K [just below $T_w(\mathrm{Ar/Na})=124.8$ K], and five values above T_w, namely, $T=126$, 127, 128, 129, and 130 K. As in the case of Li, the range $\rho^*_{sb1}\leq\rho^*_{av}\leq\rho^*_{sb2}$, where the asymmetric solutions occur diminishes for increasing temperatures. Eventually, the SSB effect disappears at $T=131$ K, which is the upper limit for T_{cpw} quoted in Table I.

Figure 7 shows Δ_N for LAS profiles in a slit of Rb with $L^*=60$ as a function of ρ^*_{av}. Data evaluated at $T=T_t$, $T=138$ K [just below $T_w(\mathrm{Ar/Rb})=138.7$ K], and three values above T_w, namely, $T=139$, 140, and 141 K are plotted. As for the substrates analyzed above, the range $\rho^*_{sb1}\leq\rho^*_{av}\leq\rho^*_{sb2}$ diminishes when the temperature is increased and the asymmetric solutions disappear at $T=141$ K, which is the upper limit for T_{cpw} included in Table I. The results for slits of K are very similar to that for Rb.

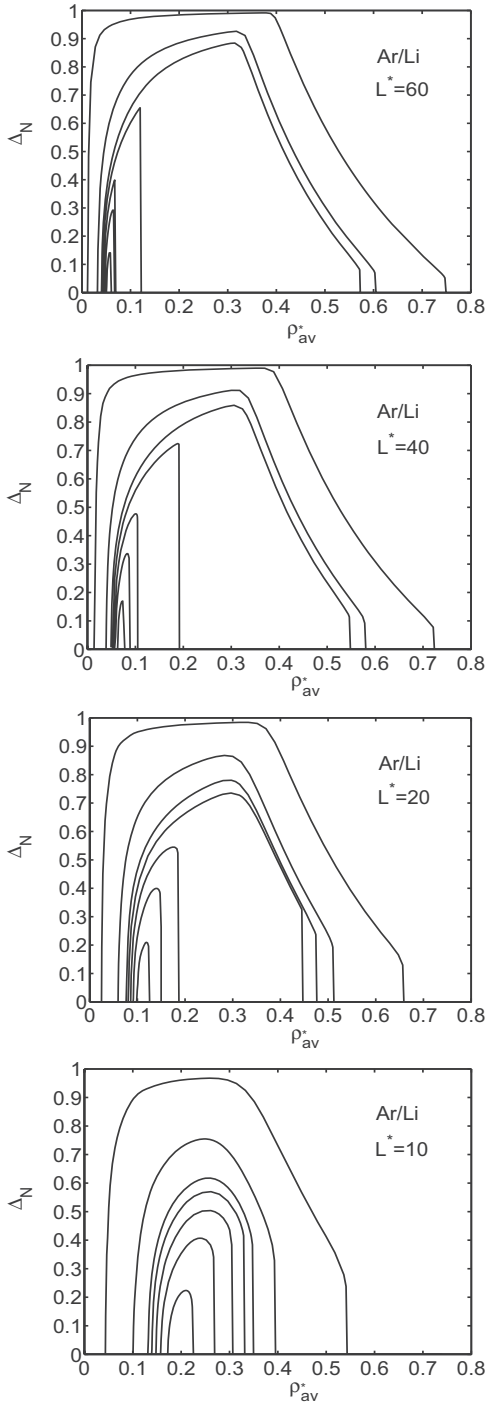

FIG. 5. Asymmetry parameter for Ar confined in slits of Li walls as a function of average density. Results for the widths $L^*=10$, 20, 40, and 60 are displayed. From outside to inside the curves correspond to temperatures $T=83.78$, 109, 114, 115, 116, 117, and 118 K. The asymmetric solutions occur for different ranges $\rho^*_{sb1}\leq\rho^*_{av}\leq\rho^*_{sb2}$.

C. Critical prewetting temperature

Let us now determine systematically the maximum temperatures T_{sb} for the occurrence of the SSB effect. We shall illustrate the procedure by describing the analysis of the data plotted in Fig. 5 for slits of different size of Li. For all the examined sizes the asymmetric solutions disappear at temperatures $T>118$ K. The critical average density $\rho^*_{av}(\mathrm{crit})$ corresponding to the peak of Δ_N at $T=118$ K for each L^* was determined, it can be cast into the form $\rho^*_{av}(\mathrm{crit})=(A/B)\tilde{\sigma}^2_{\mathrm{ArAr}}\times 10^{-2}$ Å^{-2} with $\tilde{\sigma}_{\mathrm{ArAr}}$ expressed in angstrom. For $L^*=60$ we obtained the ratio $A/B=9/16$, $A/B=17/24$ for $L^*=40$, $A/B=55/48$ for $L^*=20$, and $A/B=97/48$ for $L^*=10$. Figure 8 shows the values of $\Delta_N[\rho^*_{av}(\mathrm{crit})]$ calculated for both the LAS and RAS profiles corresponding to Ar confined between walls of Li at temperatures $T\geq T_w$. Results for slits of $L^*=10$, 20, 40, and 60 are displayed. All these data follow even rather parabolic functions. Therefore, we fitted them to sixth degree even polynomials,

This article is copyrighted as indicated in the article. Reuse of AIP content is subject to the terms at: http://scitation.aip.org/termsconditions. Downloaded to IP: 157.92.4.75 On: Fri, 26 Jun 2015 19:33:02

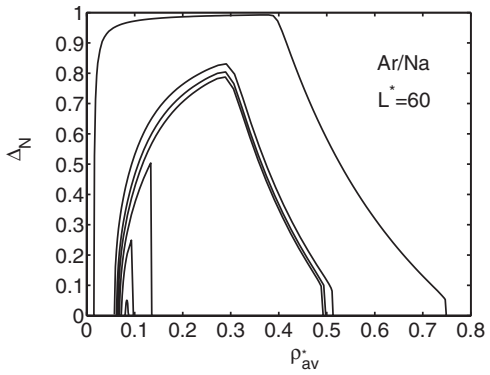

FIG. 6. Asymmetry parameter for Ar confined between two identical walls of Na located at a distance $L^*=60$ as a function of average density. From outside to inside the curves correspond to temperatures $T=83.78$, 124, 126, 127, 128, 129, and 130 K.

$$T = T_{sb} + a_2\Delta_N^2 + a_4\Delta_N^4 + a_6\Delta_N^6. \tag{3.7}$$

The results of these fits are depicted in Fig. 8. One may observe that all the fitting curves are consistent with a common value $T_{ab}=118.4$ K.

There is a general idea that the existence of g-s asymmetric profiles is a signature for nonwetting, however, we found that the SSB effect occurs for temperatures higher than T_w. It is important to emphasize that the isotherms for adsorption on a single wall indicate that on a prewetting line, at a given T, the thick films are stable only above a critical wetting coverage $n_c(cw)$. The coverage is defined as

$$n_c = \int_0^\infty [\rho(z) - \rho_B]dz, \tag{3.8}$$

where $\rho_B=\rho(z\to\infty)$ is the asymptotic bulk density which should be equal to ρ_v at a given T. Below the critical value $n_c(cw)$ the thick film is unstable and coexists with a thin one at a common chemical potential. This regime of coexistence extends from $n_c(fw)$ to $n_c(cw)$, below $n_c(fw)$ there are stable thin films. The range $\Delta n_c=n_c(cw)-n_c(fw)$ diminishes when temperature increases and becomes zero at T_{cpw}. The asymmetric solutions in a slit (like that labeled by 2 in Fig. 2) are the stable realization of the unstable regime of coexistence in the adsorption on a single wall. Our results indicate that the

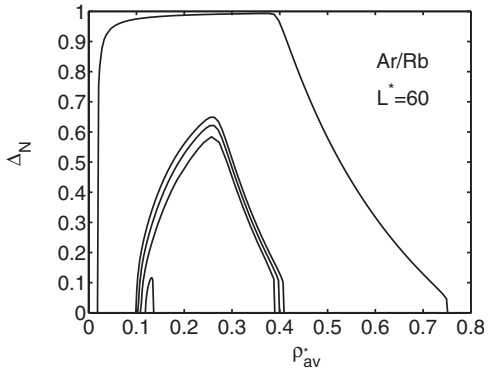

FIG. 7. Asymmetry parameter for Ar confined between two identical walls of Rb located at a distance $L^*=60$ as a function of average density. From outside to inside the curves correspond to temperatures $T=83.78$, 138, 139, 140, and 141 K.

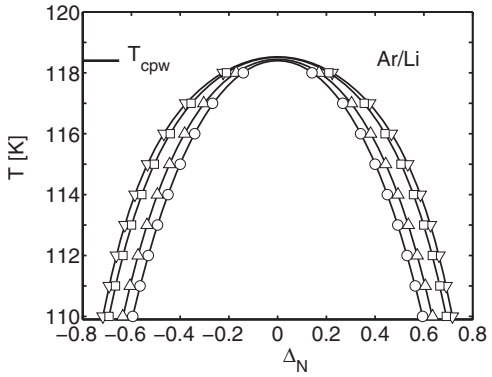

FIG. 8. Both LAS and RAS branches of the asymmetry parameter for Ar confined between walls of Li at temperatures $T\geq T_w$. Data for slits of several widths are displayed: $L^*=10$ (up-triangles), $L^*=20$ (squares), $L^*=40$ (down-triangles), and $L^*=60$ (circles). Solid curves are fits to Eq. (3.7) used for determining $T_{sb}\equiv T_{cpw}$; the obtained value is indicated by the horizontal line.

disappearance of the SSB effect coincides with the end of the prewetting line. As can be seen in Table I, the obtained value of T_{sb} for slits of Li is in agreement with the limits for T_{cpw} determined in a previous work. We are able to perform a meaningful comparison because the slits and the single walls were studied by applying the same DF theory with equal MFA. Therefore, T_{sb} may be associated to T_{cpw}.

The results for $\Delta_N[\rho^*_{av}(\text{crit})]$ calculated in the cases of the Ar/Na, Ar/K, and Ar/Rb slits were analyzed in the same way as the Ar/Li system. The obtained T_{sb} are listed in Table I. A glance at this table indicates that the values determined in the present work lay in the interval determined in the analysis of single walls in Ref. 20. We do not report results for Ar/Cs because the adsorption potential for this system is almost equal (indistinguishable in the scale of Fig. 1) to that for Ar/Rb.

IV. CONCLUSIONS

The confinement of Ar between identical planar structureless walls was studied. A series of substrates with different attractive strengths was analyzed. It was found that the profiles of Ar confined in slits of alkali metals exhibit SSB. This effect is present in a certain range of average densities $\rho^*_{sb1}\leq\rho^*_{av}\leq\rho^*_{sb2}$ already at T_t of Ar and this range diminishes for increasing temperatures. A crucial output of this work is the finding that SSB occurs above the wetting temperature T_w and disappears when a temperature $T_{sb}<T_c$ is reached. Furthermore, it was shown that by examining the evolution of the asymmetry coefficient $\Delta_N[\rho^*_{av}(\text{crit})]$ as a function of temperature one can precisely determine T_{sb}. On the other hand, it was found that the SSB effect does not occur for slits of strongly attractive walls of Mg and CO_2.

A detailed examination of the obtained T_{sb} for all the alkali metals indicates that these values fall between the lower- and upper-limit for the critical prewetting temperatures T_{cpw} established in Ref. 20 from the analysis of the adsorption on single walls. To the best of our knowledge this is the first time that such a correlation between prewetting and SSB is noticed.

Let us put our findings in a general scenario of the physisorption on planar inert walls. In Ref. 20 we found that

This article is copyrighted as indicated in the article. Reuse of AIP content is subject to the terms at: http://scitation.aip.org/termsconditions. Downloaded to IP: 157.92.4.75 On: Fri, 26 Jun 2015 19:33:02

when a fluid adsorbed on a single wall exhibits a triple-point wetting, like for Ar adsorbed on Mg and on CO_2, there is no prewetting line. In these cases the analysis of the confinement between two walls yields always symmetric profiles in the entire range of temperatures $T_t \leq T \leq T_c$ (see, e.g., Fig. 4). For systems with $T_w > T_t$, like Ar adsorbed on walls of alkali metals, there appears a prewetting line where there is a coexistence of thin and thick films which cannot be seen together in only one profile. Both these films become equal at T_{cpw}. When studying the confinement of the latter kind of systems below T_w in a slit geometry, one always gets a regime of average density where there are asymmetric solutions. The existence of asymmetric g-s extends above T_w up to a critical temperature T_{sb} which coincides with T_{cpw}. In this regime of temperature the confined fluid exhibits in one profile the coexistent thin and thick films (see profile 2 in Fig. 2). We conjecture that the coincidence of T_{sb} and T_{cpw} is not fortuitous, but it is a signature indicating that the same phenomenon is simultaneously occurring in both geometries. Namely, that the conditions for complete wetting are reached at the same temperature.

Regarding a future work, let us mention that Berim and Ruckenstein[31] found that under certain circumstances the symmetry on the *x*-*y* plane might be broken. We are planning to search for this kind of symmetry breaking in realistic systems. When preparing the final version of the present paper, we became aware that Berim and Ruckenstein[32] found that the SSB effect also occurs in the case of the quantum fluid ^{4}He confined between identical walls of Cs.

We hope that the present theoretical results could encourage some experimental groups to try to perform measurements of adsorption for the described systems in slit geometries.

ACKNOWLEDGMENTS

This work was supported in part by Grant No. PICT 31980/05 from Agencia Nacional de Promoción Científica y Tecnológica and Grant No. X099 from Universidad de Buenos Aires, Argentina.

[1] L. W. Bruch, M. W. Cole, and E. Zaremba, *Physical Adsorption: Forces and Phenomena* (Dover, Mineola, NY, 2007).
[2] C. Rascón and A. O. Parry, Nature (London) **407**, 986 (2000).
[3] A. F. Bakker, Thesis, Technische Universiteit Delf, 1983.
[4] A. F. Bakker and C. Bruin, in *Special Purpose Computers*, edited by B. J. Alder (Academic, London, 1988).
[5] J. H. Sikkenk, J. O. Indekeu, J. M. J. van Leeuwen, and E. O. Vossnack, Phys. Rev. Lett. **59**, 98 (1987).
[6] J. H. Sikkenk, J. O. Indekeu, J. M. J. van Leeuwen, E. O. Vossnack, and A. F. Bakker, J. Stat. Phys. **52**, 23 (1988).
[7] M. J. P. Nijmeijer, C. Bruin, A. F. Bakker, and J. M. J. van Leeuwen, Physica A **160**, 166 (1989).
[8] M. J. P. Nijmeijer, C. Bruin, A. F. Bakker, and J. M. J. van Leeuwen, Phys. Rev. A **42**, 6052 (1990).
[9] M. J. P. Nijmeijer, C. Bruin, A. F. Bakker, and J. M. J. van Leeuwen, Phys. Rev. B **44**, 834 (1991).
[10] G. O. Berim and E. Ruckenstein, J. Phys. Chem. B **111**, 2514 (2007).
[11] G. O. Berim and E. Ruckenstein, J. Chem. Phys. **126**, 124503 (2007).
[12] C. Ebner and W. F. Saam, Phys. Rev. Lett. **38**, 1486 (1977); W. F. Saam and C. Ebner, Phys. Rev. A **17**, 1768 (1978).
[13] L. Szybisz and S. A. Sartarelli, J. Chem. Phys. **128**, 124702 (2008).
[14] S. A. Sartarelli, L. Szybisz, and I. Urrutia, Int. J. Bifurcation Chaos Appl. Sci. Eng. (to be published).
[15] S. A. Sartarelli and L. Szybisz, Papers in Physics **1**, 010001 (2009); e-print arXiv:0909.2244.
[16] A. Chizmeshya, M. W. Cole, and E. Zaremba, J. Low Temp. Phys. **110**, 677 (1998).
[17] G. Mistura, F. Ancilotto, L. Bruschi, and F. Toigo, Phys. Rev. Lett. **82**, 795 (1999).
[18] P. J. Marshall, M. M. Szczęśniak, J. Sadlej, G. Chałasiński, M. A. ter Horst, and C. J. Jameson, J. Chem. Phys. **104**, 6569 (1996).
[19] S. A. Sartarelli, L. Szybisz, and I. Urrutia, Phys. Rev. E **79**, 011603 (2009).
[20] S. A. Sartarelli and L. Szybisz, Phys. Rev. E **80**, 052602 (2009).
[21] R. Pandit, M. Schick, and M. Wortis, Phys. Rev. B **26**, 5112 (1982).
[22] P. I. Ravikovitch, A. Vishnyakov, and A. V. Neimark, Phys. Rev. E **64**, 011602 (2001).
[23] F. Ancilotto, S. Curtarolo, F. Toigo, and M. W. Cole, Phys. Rev. Lett. **87**, 206103 (2001).
[24] E. Kierlik and M. L. Rosinberg, Phys. Rev. A **42**, 3382 (1990).
[25] J. D. Weeks, D. Chandler, and H. C. Andersen, J. Chem. Phys. **54**, 5237 (1971).
[26] V. A. Rabinovich, A. A. Vasserman, V. I. Nedostup, and L. S. Veksler, *Thermophysical Properties of Neon, Argon, Krypton, and Xenon* (Hemisphere, Washington, D.C., 1988).
[27] S.-T. Wu and G.-S. Yan, J. Chem. Phys. **77**, 5799 (1982).
[28] A. Trokhymchuk and J. Alexandre, J. Chem. Phys. **111**, 8510 (1999).
[29] A. Maciołek, R. Evans, and N. B. Wilding, J. Chem. Phys. **119**, 8663 (2003).
[30] P. G. de Gennes, Rev. Mod. Phys. **57**, 827 (1985).
[31] G. O. Berim and E. Ruckenstein, J. Chem. Phys. **128**, 024704 (2008).
[32] G. O. Berim and E. Ruckenstein, J. Chem. Phys. **131**, 184707 (2009).

This article is copyrighted as indicated in the article. Reuse of AIP content is subject to the terms at: http://scitation.aip.org/termsconditions. Downloaded to IP: 157.92.4.75 On: Fri, 26 Jun 2015 19:33:02